Ore Geology Reviews 76 (2016) 268–279

Contents lists available at ScienceDirect

Ore Geology Reviews

journal homepage: www.elsevier.com/locate/oregeorev

# Multi-stage enrichment processes for large gold-bearing ore deposits

Sebastien Meffre [a,*], Ross R. Large [a], Jeffrey A. Steadman [a], Daniel D. Gregory [a], Aleksandr S. Stepanov [a], Vadim S. Kamenetsky [a], Kathy Ehrig [b], Robert J. Scott [a]

[a] ARC Centre of Excellence in Ore Deposits (CODES), University of Tasmania, Private Bag 79, Hobart, Tasmania 7001, Australia
[b] BHP-Billiton, GPO Box 1777, Adelaide, South Australia 5001, Australia

ARTICLE INFO

*Article history:*
Received 6 January 2015
Received in revised form 26 August 2015
Accepted 1 September 2015
Available online 11 September 2015

*Keywords:*
Gold
Hydrothermal ore deposit
Multistage
Giant ore deposits

ABSTRACT

A review of previous studies of the world's large hydrothermal gold deposits indicates that the largest deposits tend to show complicated parageneses where multiple gold enrichment events and processes have been involved in the deposit generation. These observations suggest that multistage processes may even be a requirement for the formation of large deposits. In some deposits (e.g. Witwatersrand, Boddington Cadia, Sukhoi Log or Carlin) the different enrichment processes occur millions of years apart. In others, such as many large porphyry deposits, the different stages are much closer in time. In many deposits, particularly sedimentary-hosted deposits, early diffuse enrichment occurs within a particular province that is then upgraded by more focused processes (e.g., Sukhoi Log; Kalgoorlie). The presence of this early diffuse enrichment could explain the tendency for gold deposits to cluster into camps.

This model has important implications, as the presence or absence of multiple gold events could be used to discriminate, at the exploration and feasibility stages, between small deposits with single stage ore genesis and more complicated deposits with multistage enrichment and the potential for larger gold endowment.



## 1. Introduction

Large gold deposits (>10 million ounces Au) are rare geological feature and are formed by either:

1. A single unusual event.
2. An exceptional set of combined circumstances.

Previous studies reviewing the spectrum of large metallic deposits (Emsbo et al., 2006; Richards, 2013; Laznicka, 2014) suggest that the giant metallic ore deposits are not exceptional in their processes but circumstances have combined to form a much larger deposit than would otherwise exist. Part of the evidence cited for this is that very large deposits are not far outliers but rather conform to the overall characteristics of deposits in their class worldwide. The largest deposits are within the overall log-normal distribution of deposits in terms of grade (Fig. 1a) and continue the power law distribution in terms of size (Fig. 1b). In this study we review existing data from some of the world's largest gold deposits to elucidate whether the circumstances which led to gold enrichment were different from similar processes in smaller deposits. The impetus for this paper originates from various studies of gold deposits by the authors, where empirical observations suggested that the largest gold deposits tended to have very complicated multistage ore parageneses compared with smaller deposits. The exploration strategies that can be used to find new gold ores will necessarily differ depending on whether a single event or multiple events are involved. For example, in single-stage systems, searches should concentrate on the area near a discrete source region using a simple source-pathway-trap model. In the multi-stage systems a much more probabilistic strategy should be employed, involving the identification of multiple ore systems that overlap in space.

The origin of gold deposits has been the subject of considerable debate and remains controversial to this day. Most published ore deposit models in the literature to date involve gold being sourced from the mantle, the lower crust or the upper crust (Groves, 1993; Phillips and Powell, 2010; Thomas et al., 2011; Hronsky et al., 2012; Tomkins, 2013) transferred to hydrothermal fluids which carry the gold into a zone with a strong chemical (pH or Eh) or physical (temperature or pressure) contrast, leading to the deposition of gold in veins or within other minerals (particularly pyrite). Gold deposits are generally subdivided into a number of different styles based on the mineralogy and geometry of mineralisation and the rocks in which they occur. Within each type there are considerable variations and gradations.

Some studies of gold mineralization have proposed more complex models, requiring the formation of multiple vein arrays, mixing of isotopic sources and overprinting of alteration zones (e.g. Nichols and Hagemann, 2014), (e.g. Nichols and Hagemann, 2014). Complex relationships are particularly well-documented in forensic-type studies which use micro-analytical techniques such as electron, laser, X-ray, proton and ion beam techniques to study minerals and alteration

* Corresponding author.
*E-mail address:* smeffre@utas.edu.au (S. Meffre).

http://dx.doi.org/10.1016/j.oregeorev.2015.09.002
0169-1368/

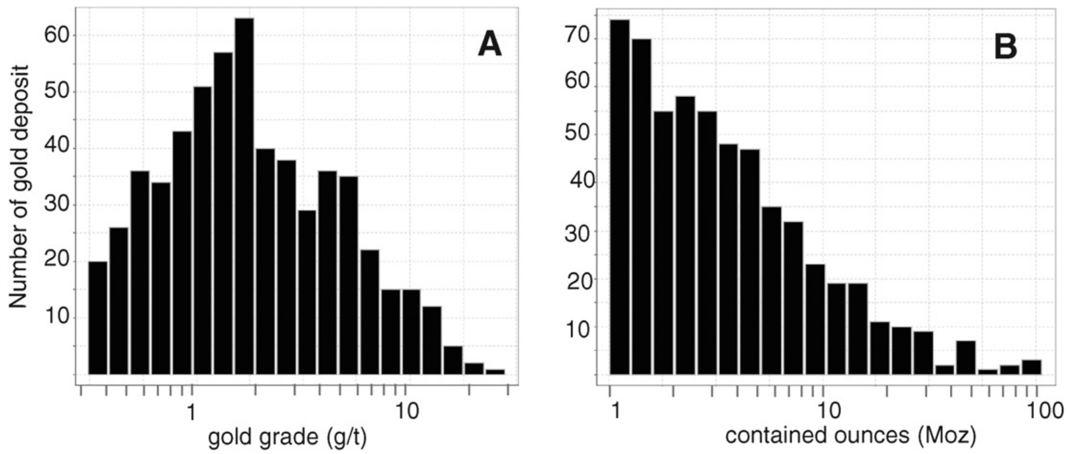


**Fig. 1.** Histograms showing the log normal distribution of gold deposit grades and power law distribution of gold deposit size (resource for deposits >1 Moz). Data from NRH Research — 2013 Ranking Gold Mines & Deposits (http://www.visualcapitalist.com/wp-content/uploads/2013/11/global-gold-mine-and-deposit-rankings-2013.pdf).

zones within ore deposits (Oberthür et al., 1997; Large et al., 2009; Sung et al., 2009). These tend to show that the gold enrichment processes are protracted and in many cases more than one enrichment event has been documented. In some, there is evidence for early low-grade enrichment followed by a late high-grade overprint. In others, the scientific literature is divided as to whether the early or late events were responsible for the enrichment (e.g. the long running Witwatersrand debate; Large et al., 2013).

This paper briefly summarizes the some of the existing geological information for most of the world's large gold deposits with a view to comparing and contrasting gold enrichment processes in a number of different deposit styles to determine whether gold is introduced by a single discrete event or by a particular combination of events and circumstances. This paper is in no way comprehensive but outlines some of the temporal evidence for multistage gold concentration processes in some large deposits within a range of deposit styles. The paper focuses in particular on deposits on which the authors have worked over the last decade. Although this introduces a particular bias, we would argue that these sites are at least partially representative of large gold deposits worldwide (Fig. 2).

## 2. Witwatersrand

The Witwatersrand basin contains numerous strata-bound high grade gold deposits which are characterized by complex parageneses. Despite the very low metamorphic grade and the relatively undeformed nature of the 2.9–2.7 Ga host sedimentary rocks, no consensus has been reached on the source of the gold or the enrichment mechanisms. Some studies emphasize the presence of early detrital gold and early gold in pyrite in discrete conglomeratic horizons (e.g. Minter, 1999) while others focus on the hydrothermal alteration and the late introduction of the majority of the gold (Law and Phillips, 2006; Phillips and Powell, 2015). Some recent studies present models showing both early gold enrichment followed by the late re-introduction of gold (Mathur et al., 2013) with the earlier event cross-cut (Agangi et al., 2015) and overprinted by late stage overgrowth (Large et al., 2013) (Fig. 3). However, there is no consensus as to how much of the gold was introduced in the early stage and the amount added during the late hydrothermal overprint. It is difficult to see how these estimates of relative importance could be obtained using existing techniques. One problem with providing this type of estimate for the Witwatersrand deposits is that, as in

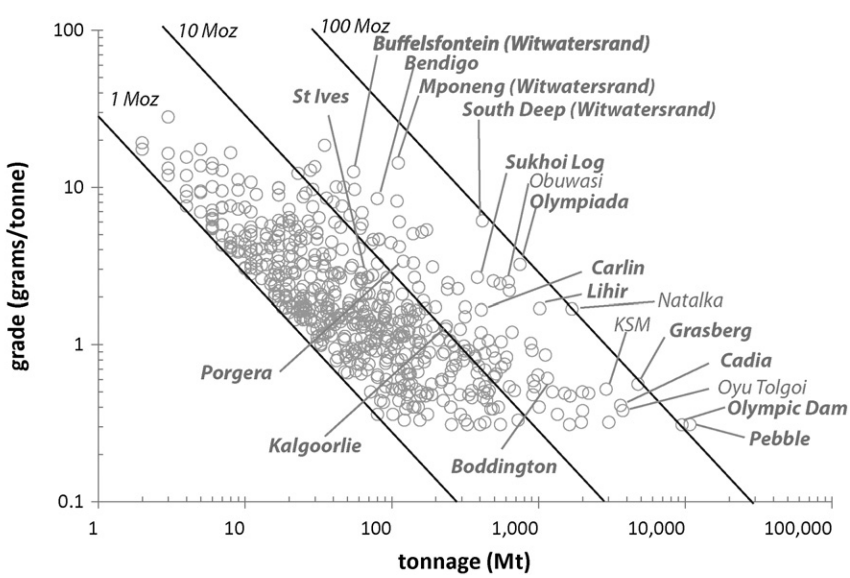


**Fig. 2.** Deposit size and grade, showing the deposits discussed in the text. Data as for Fig. 1 except for Olympic Dam (9833 Mt at 0.31 g/t; Kathy Ehrig, BHP pers. Com. 2014) and Bendigo (historical resource: 22 Moz at 8 g/t estimated from documents at http://www.unitymining.com.au/bendigo-goldfield-history/). Mines labeled in bold text are those discussed in the text.

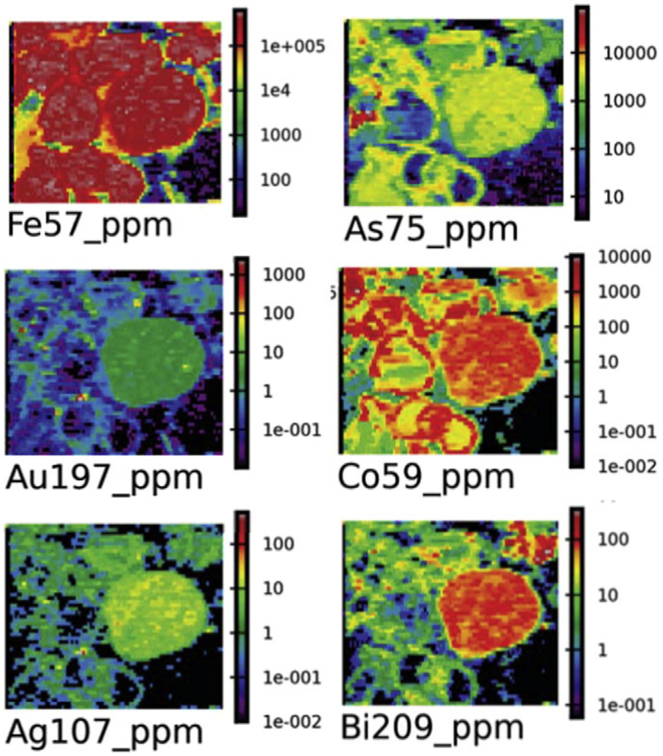


**Fig. 3.** Laser ablation mass spectrometry images of pyrite from the Witwatersrand carbon leader reef, Tautona Mine. Rounded Fe-rich zones are detrital pyrites. The large right of centre detrital pyrite is enriched in early stage invisible gold (~5 ppm) plus As, Co, Bi & Ag, with Ag/Au > 1. The second stage gold event is marked by the overgrowth rims outlined by Au–As enrichment, with Ag/Au < 1. Note the free gold grains on pyrite rims marked by the red and yellow spots on the Au image. Image is 4 mm across.

many deposits worldwide, gold is easily mobilized. At the sub-millimeter scale it is possible to show this mobilization (Agangi et al., 2015); however, beyond a few meters it becomes very difficult to establish what constitutes re-introduction from another source and what constitutes re-mobilization. Irrespective of the relative weighting placed on the early or late events, it is clear that at least two events were involved in the formation of the Witwatersrand deposits and that these events occurred almost 1 billion years apart. Both major events are now well-dated with a strong agreement between the various radiogenic isotopic systems including

- 3100–2800 Ma for model Pb ages on the early gold-rich pyrite (Barton and Hallbauer, 1996; Poujol et al., 1999; Large et al., 2013).
- 3030 Ma for Re–Os isochron age for early pyrite and gold particles (Kirk et al., 2001) 3030 Ma for Re–Os isochron age for early pyrite and gold particles.
- 3100–2600 Ma and 2200–2000 Ma U–Pb ages for xenotime associated with ores (England et al., 2001; Kositcin et al., 2003).
- 2000–2100 Ma Pb-Pb isochrons on late pyrite rims containing small gold inclusions (Poujol et al., 1999; Large et al., 2013).
- 2140–2030 Ma U–Pb ages for hydrothermal monazite associated with ores (Rasmussen et al., 2007) 2050 Ma mixing trends of initial Os in sulfides (Mathur et al., 2013).

## 3. Kalgoorlie

The Kalgoorlie goldfield encompasses two physically separate gold deposits, the Golden Mile and Mt. Charlotte (Travis et al., 1971; Phillips, 1986; Clout, 1989; Clout et al., 1990; Nixon et al., 2014). The Golden Mile is characterized by narrow quartz-carbonate breccia zones containing locally abundant free gold and gold–silver telluride, with a 1–5 mm halo of fine-grained auriferous pyrite–sericite–ankerite ± tourmaline. These structures have historically been termed 'Golden-Mile' or 'Fimiston' lodes. Some of the Fimiston lodes can have a dark green color due to the presence of V-bearing micas and other V-rich minerals (Nickel, 1977). These unique and enigmatic variants of the Fimiston system are termed 'Green Leader' lodes, and they are exceptionally high grade (commonly several oz./t average Au; Tomich, 1986). The Mt. Charlotte deposit, 3 km north of the Golden Mile Super Pit, is a quartz stock work vein system with a total Au endowment of ~8 Moz at 4 g/t average grade (Ridley and Mengler, 2000). The veins in this system can be wide (i.e., 1–2 m), but unlike the finer-grained quartz in the Fimiston lodes, the quartz in them is coarse-grained and commonly bucky. Gold is primarily found as inclusions in medium-coarse grained euhedral pyrite, which is part of a vein-proximal pyrite–ankerite alteration selvage; only minor free gold exists in the quartz veins themselves, and tellurides are rare. In both deposits, the primary host for ore is the Golden Mile Dolerite, a texturally and chemically zoned mafic unit historically described as a shallow intrusive sill (Travis et al., 1971). At the Golden Mile Super Pit, both mineralization styles (i.e., vein breccias and vein stockworks) are present, with the latter cross-cutting the former. However, only the stockworks are present at the Mt. Charlotte mine.

A recent study has also highlighted the presence of early gold-bearing (up to 5 ppm) pyrite nodules which predate deformation and ore formation and have distinct Pb and S isotopic signatures relative to both ore styles (Steadman and Large, 2014; Steadman et al., 2015). These represent the first Au "event" at Kalgoorlie. The question of their involvement in the ore-forming processes at Kalgoorlie is not strictly within the purview of this paper, but we note here that, given the presumed thickness of the main nodule-rich shale units at Kalgoorlie (i.e., the Kapai Slate and Oroya Shale, max thickness 60 m), there is insufficient material for them to produce the Golden Mile lodes on their own. Nevertheless, they, along with the younger (and significantly thicker) Black Flag Group, were present at Kalgoorlie at least 20 Ma before the later ore-forming events likely began.

The difference in the absolute timing of the various mineralisation events at Kalgoorlie is somewhat controversial (Bateman and Hagemann, 2004; McNaughton et al., 2005; Vielreicher et al., 2010; Vielreicher et al., 2015). A recent review of absolute timing relationships between the two dominant ore styles at Kalgoorlie found that the Fimiston/Oroya-style vein breccia shoots and Mt. Charlotte-style quartz-vein stockworks formed broadly at the same time (2.64 Ga) but that localized hydrothermal activity also led to some gold mineralization or remobilization during brittle deformation at 2.61–2.60 Ga (Vielreicher et al., 2015). At present uncertainty on the difference in the timing remains relatively large (up to 20 Ma Vielreicher et al., 2014) such that, in the absence of clear cross-cutting field relationships, one could legitimately interpret the Mt. Charlotte ore style as predating the Fimiston/Oroya Au–Te lodes. As age-dating techniques continue to improve, the error bars on age dates from the Neoarchean will doubtless shrink such that realistic interpretations of age data from this district can be made as a matter of course.

## 4. St. Ives

The St. Ives gold deposit is located approximately 60 to 80 km south of Kalgoorlie within the Eastern Goldfields super terrane. The gold is hosted predominantly by dolerite, and mafic and ultramafic volcanic and volcaniclastic rocks of the Kambalda sequence. Two different gold deposition ages have been identified by previous studies, 2630 Ma (Nguyen, 1997) and 2655 +/− 13 Ma (by analogy as dates are from contemporaneous structures developed 60 km to the north) (Rasmussen et al., 2009).As with the nearby Kalgoorlie deposits, the earliest gold-bearing minerals are diagenetic pyrite from the Kapai Slate which has an order of magnitude more gold (Gregory, 2014) than the median of gold values of diagenetic pyrite (Gregory et al., 2014). The main gold mineralisation event probably occurred in a regional sinistral transpression event associated with NNW faults (Blewett et al., 2010; Miller et al., 2010) but earlier intrusion of porphyries during the southwest to northeast-directed regional extension also may also have contributed to mineralisation (Miller et al., 2010). The final gold mineralizing event is related to southwest to northeast regional compression, although the extent of the mineralization from this event is thought to be minor at St. Ives and much more significant at Mt. Charlotte in the Kalgoorlie area (Blewett et al., 2010). In addition to multiple periods of gold enrichment in the St. Ives gold district there is also evidence for different sources of metals and metal transport mechanism. Proposals include:

1. Gold carried by fluids derived from devolatilisation at depth during metamorphism (Phillips and Powell, 2010).

2. Gold carried in relatively high temperature, oxidized, F- and K-bearing fluids derived from a proximal magmatic source (Bath et al., 2013) which mixed with a more reduced fluid (Neumayr et al., 2008).

Although these models have been proposed as alternative models to explain mineralisation the complexity of the structural and chemical processes of mineralisation in this deposit strongly suggests that more than one mechanism may responsible for mineralisation.

## 5. Sukhoi Log

Sukhoi Log is a large orogenic gold deposit in Siberia, Russia, situated to the north of Lake Baikal. The ore is hosted in the hinge of a large anticlinal structure in a mixed fine-grained siliciclastic rock and carbonate sequence (Large et al., 2007a; Large et al., 2007b). Gold is associated with quartz and pyrite. There is evidence for progressive recrystallisation and concentration from low grade gold inclusions in pyrite which are either <0.1 μm in size or the gold is dissolved in the lattice of the early pyrite, to higher grade late stage overgrowth and recrystallized pyrite associated with larger visible gold inclusions. Typical of many deposits, the early stage syn-diagenetic pyrite has a high Ag/Au ratio, whereas the later stage early metamorphic pyrite has a lower Ag/Au ratio (Large et al., 2007a; Large et al., 2007b). The Pb isotopic composition changes with each successive stage of gold-bearing pyrite, suggesting genesis over successive stages in a 100–150 Ma period between the Late Neoproterozoic and the Cambrian (Meffre et al., 2008). Other minerals, such as large authigenic monazite also track fluid flow and formation over a similar period with the core of the monazite recording early fluid flow at 573 ± 13 Ma and the higher temperature rims recoding fluid flow at 509 ± 10 Ma (Meffre et al., 2008). The monazite and Pb isotopic data is supported by Re–Os data at both this deposit and the related giant (77 Moz) Olympiada deposit (same age, fold belt and mineralisation style) (Yakubchuk et al., 2014). The Olympiada deposit has not been studied in as much detail as Sukhoi Log but a pilot the Re-Os study concluded that disturbance of the Re system possibly suggested more than one generation of sulfide and that the generations formed at distinctly different times.

## 6. Bendigo

The Bendigo deposit is a giant saddle reef quartz-vein system hosted by Ordovician turbidites in the Victorian Goldfield area, southern Australia. Recent research by Thomas et al. (2011), based on laser ablation mass spectrometric (LA–ICPMS) element mapping of pyrite in the veins and host rocks, has demonstrated a two-stage process of formation. The first stage involves pre-concentration of gold in pyrite within carbonaceous shales which form the tops of turbidite units. The laser mapping (Fig. 4) showed diagenetic pyrite in the shales with average gold contents of 600 ppb, 1300 ppm As, Ag/Au > 1, and high levels of Mn, Zn, Mo, Cu, Ni and Cd. This represents a gold enrichment factor of 3 when compared to normal black shale pyrite (e.g. modern pyrite from sediments, 0.2 ppm, Gregory et al., 2014; Large et al., 2014; Large

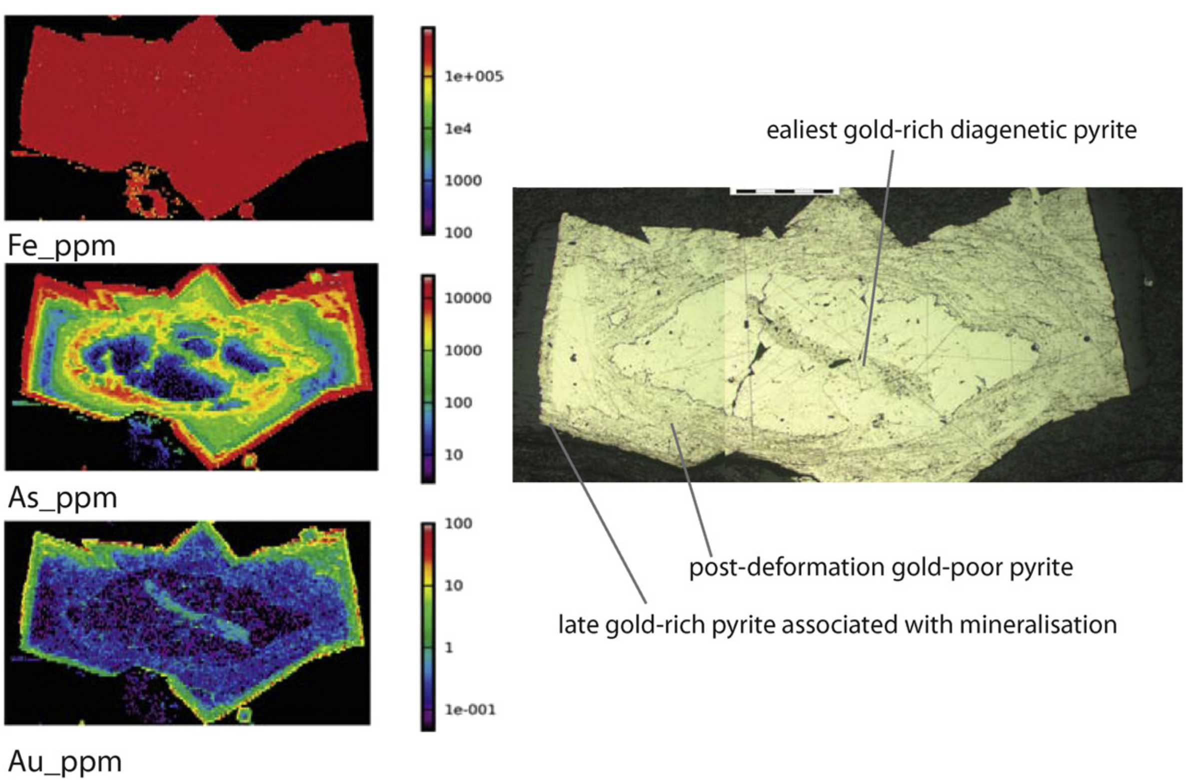


**Fig. 4.** Laser ablation mass spectrometry images of pyrite from Bendigo showing the early Au-rich pyrite overgrown by low Au pyrite followed by late high Au pyrite modified from (Large et al., 2009). Image is 3 mm across (Fig. 4). Laser ablation mass spectrometry images of pyrite from Bendigo showing the early Au-rich pyrite overgrown by low Au pyrite followed by late high Au pyrite modified from Large et al. (2009). Image is 3 mm across.

et al., 2015). The second stage involved the introduction of an Au–As-rich fluid during orogenesis, with maximum gold input at the final stage of flow, forming Au–As-rich rims on pre-existing pyrite (Ag/Au < 1) and introducing free gold into the quartz vein saddle reefs. This second process amounted to a further gold enrichment of around 200 times. Thomas et al. (2011) suggested the source of the second stage gold fluid was from deeper in the basin, where sedimentary arsenian pyrite was converted to pyrrhotite, releasing Au and As into the metamorphic fluid. The first stage gold concentration occurred during and immediately after sedimentation, around 470 Ma with early pyrite forming in the top few centimeters to meters below the sea floor as well as deeper down during diagenesis. The second stage followed 30 million years later during orogenesis (443 ± 3 Ma Phillips et al., 2012). Laser ablation Pb isotopic analyses (unpublished data) show distinct differences between the inner and outer zones consistent with this timing. The mass balance calculations undertaken at this deposit (Thomas et al., 2011) suggest that the gold at this deposit could be concentrated from a 7 × 20 × 2.7 km volume of black shale within the goldfields themselves during orogenesis. This volume is relatively small relative the extent of the carbonaceous Early Paleozoic rocks in this area.

## 7. Carlin

The Carlin province in northeast Nevada is one of the largest gold-producing districts in the world, with historic production and reserves of gold exceeding 6000 t (193 Moz, Emsbo et al., 2006). The province hosts numerous gold deposits ranging in age from Devonian to Miocene (Emsbo et al., 2003; Emsbo et al., 2006), but is best known for Eocene Carlin-type disseminated gold deposits. These are primarily hosted by carbonate-rich Paleozoic miogeoclinal sedimentary rocks (Cline et al., 2005), and range from small to very large (e.g. the 40 Moz Post-Betze-Screamer deposit), and low to very high grade (e.g. 25 g/t Au Meikle deposit). Gold in Carlin-type deposits is almost exclusively contained in the crystal lattice of very fine-grained arsenian pyrite, which commonly forms very narrow rims on earlier hydrothermal and diagenetic pyrite (Cline et al., 2005; Reich et al., 2005; Barker et al., 2009). Carlin-type pyrite contains 1 to >10 wt.% As and several hundred to several thousand parts per million (and rarely, percent levels) of Au, Sb, Tl and Hg. Gold to silver ratios generally exceed 10 and base metal contents are typically low (Emsbo et al., 2003; Emsbo et al., 2006). These traits help distinguish Carlin-type deposits from other gold deposit types developed in the province (e.g. Figs. 5 and 6; Emsbo et al., 1999; Emsbo et al., 2003; Emsbo et al., 2006; Nutt and Hofstra, 2007)..

Formation of the Carlin-type deposits was broadly coincident in space and time with Eocene crustal extension and magmatism (Cline et al., 2005; Emsbo et al., 2006; Ressel and Henry, 2006), and both processes were potentially important for driving hydrothermal fluid flow during mineralisation. However, the apparent restriction of Carlin-type deposits, and indeed most other gold deposits in the region, to a series of well-defined linear belts, or 'trends', reflects the long-lived influence (and episodic reactivation) of basement faults along the Neoproterozoic rifted margin of western North America, which underlies the Carlin province (Crafford and Grauch, 2002; Emsbo et al., 2006). During the middle Devonian, reactivation of basement faults is interpreted to have caused localized discharge of Au-rich, reduced, basinal brines, resulting in both discordant and stratiform sedimentary exhalative (sedex) gold mineralization on the north Carlin trend (Emsbo et al., 1999; Emsbo et al., 2003; Emsbo et al., 2006). Sedex gold ore in the upper zone of the Rodeo deposit grades up to 68 g/t Au, and anomalous gold (0.2–3 ppm Au) occurs at this stratigraphic level over an area of >30 km$^2$ around the deposit. The spatial proximity of Devonian gold mineralized zones on the north Carlin trend to some of the largest and highest grade Carlin-type deposits ever discovered (e.g. the Meikle deposit is partly superimposed on the sedex plumbing system), led (Emsbo et al., 1999) to suggest that gold introduced during the Devonian may have been remobilized and upgraded during later hydrothermal events, and most importantly, during the Eocene. Emsbo et al. (2000) also reports the presence of Jurassic mineralisation in localized areas along the trend.

It is impossible to precisely quantify the amount of gold introduced to the north Carlin trend during Devonian sedex gold mineralisation; and indeed, what proportion was exhaled at the sea floor and what was deposited at various depths along the underlying plumbing system. The fine grained and cryptic nature of the stratiform ores, and the widespread occurrence of Carlin-type overprints, means there will always be some uncertainty about how much of the gold that now resides at this stratigraphic level is related to Devonian mineralization. Nonetheless, given the very high grades of some sedex ores unaffected by Carlin-type hydrothermal overprints, and the thickness (>10 m), average gold content (0.2–3 ppm Au) of the stratiform horizon around the Rodeo deposit, it is plausible that >5–10 Moz of gold (mostly below ore grade) was originally deposited on the sea floor within several kilometers of the vent site near Rodeo. Although the amount of in situ sedex gold mined represents a small fraction of the total production on the Carlin trend, gold introduced during Devonian appears a major factor in the overall endowment of the district.

## 8. Olympic Dam

The Olympic Dam Fe-oxide copper uranium gold silver deposit, located on the Stuart Shelf in South Australia, is one of the world's largest gold resources (Fig. 1). However, gold is a by-product which accounts for approximately 5% of the operations revenue. The deposit occurs in the tectono-magmatic hydrothermal Olympic Dam Breccia Complex which is hosted within the ~1590 Ma Roxby Downs Granite (Skirrow et al., 2007), part of the regionally extensive Mesoproterozoic Gawler silicic large igneous province (McPhie et al., 2011a). The deposit is unconformably overlain by ~320 m of undeformed Neoproterozoic to Cambrian and younger sedimentary rocks (McPhie et al., 2011b). The unconformity represents a time break of ~1000 million years. Gairdner Dyke Swarm (~820 Ma) dolerite to basaltic dykes (Huang et al., in press) and Delamerian age (~510 Ma) barite–fluorite–siderite dykes (Maas et al., 2011) cross cut the Olympic Dam Breccia Complex and Roxby Downs Granite.

The dominant components of the Olympic Dam Breccia Complex are derived from weak to intensely brecciated Roxby Downs Granite. Other lithologies consist of bedded clastic facies units, felsic volcanic fragments and mafic-ultramafic dykes. These components have been weakly to intensely altered to Fe-oxides and sericite ±, chlorite, siderite, fluorite, and barite.

Sulfides (pyrite, chalcopyrite, bornite, and chalcocite) occur disseminated throughout the breccias and likely formed during the waning stages of brecciation. Sulfide veins are rare. Pyrite and chalcopyrite formed relatively early and are associated with both $Fe^{+2}$ and $Fe^{+3}$ bearing alteration minerals while bornite and chalcocite are texturally later than pyrite-chalcopyrite and are strongly associated with hematite. Uranium minerals (uraninite, coffinite, brannerite) are also disseminated throughout breccias, but also occur in veins. Gold occurs as ~1–20 μm sized grains of electrum (variable Au–Ag–Cu–Fe composition), calaverite, petzite and tetra-auricupride; however, rare large nuggets and bonanza veins are present along relatively late stage structures. Gold also occurs as sub-microscope grains in pyrite and chalcopyrite and to a significantly lesser extent in bornite and chalcocite. Approximately 70% of the gold is associated with the sulfides, with the remaining 30% mainly with sericite, barite and quartz. Electrum associated with the sulfides differs both compositionally and morphologically from electrum associated with non-sulfide gangue minerals.

Based on recent and in continuing studies of Pb–Pb, Sm–Nd and Rb–Sr isotopic dating of Olympic Dam hydrothermal minerals, including uraninite, there is strong evidence for multiple U and rare earth element mineralization events post-1590 Ma, possibly as young as the Paleozoic

(Meffre et al., 2010; Maas et al., 2011). The complex hematite paragenesis and textural evolution (Ciobanu et al., 2013b), the Re–Os dating of the ore (McInnes et al., 2008) and the cross-cutting nature of some of the high gold intervals all suggest that some of the bornite, chalcocite, hematite and gold may have also precipitated much later than 1590 Ma.

## 9. Boddington

The Boddington deposit is an Archean gold deposit in southwestern Australia. Although the authors have not worked on this deposits, the deposit is large and its ore has well-dated sulfide generations deposited over 80 Ma with postulated successive addition of gold from a number of different events and sources (Ciobanu et al., 2013a). The gold is hosted by in series of steeply-dipping veins containing quartz, molybdenite, chalcopyrite, carbonate, gold-bearing pyrite and gold minerals which postdate earlier chalcopyrite and molybdenite mineralisation (Allibone et al., 1998; McCuaig et al., 2001). Detailed work on the molybdenite including Re–Os dating (Stein et al., 2001) and laser ablation mass spectrometer trace element characterization (Ciobanu et al., 2013a) has shown that the early and late mineralisation have very different ages (2707 ± 17 Ma and 2623 ± 9 Ma) and different trace element characteristics. The trace element characteristics in the molybdenite, the mineralogy of the mineral and the age of nearby intrusions suggest that the early mineralisation is of porphyry origin.

## 10. Porphyry deposits

Many of the largest porphyry deposits worldwide show a duality in their mode of formation either with epithermal mineralisation superimposed on earlier porphyry mineralisation (Sillitoe, 1994; Richards, 2013) or multiple magmatic events contributing to the metal budgets giving rise to protracted mineralisation over a significant time interval (e.g. 1–18 Ma; Wilson et al., 2007; Sillitoe and Mortensen, 2010; Lang et al., 2013). A previous study has observed that "Telescoped systems are believed to possess greater potential for the existence of both porphyry-type deposits at shallower than normal depths and giant ore deposits" (Sillitoe, 1994); (Sillitoe, 1994) proposing that deposits with multiple stages of mineralisation may be more prospective for high grades and large endowment that those with only a single stage.

Examples of large porphyry deposits which show multistage mineralisation include the Lihir gold deposit (Papua New Guinea) (Sillitoe, 1994; Blackwell, 2010; Blackwell et al., 2014) the Pebble Cu–Au–Mo porphyry, Alaska and Porgera Au–Ag–Zn–Pb (Papua New

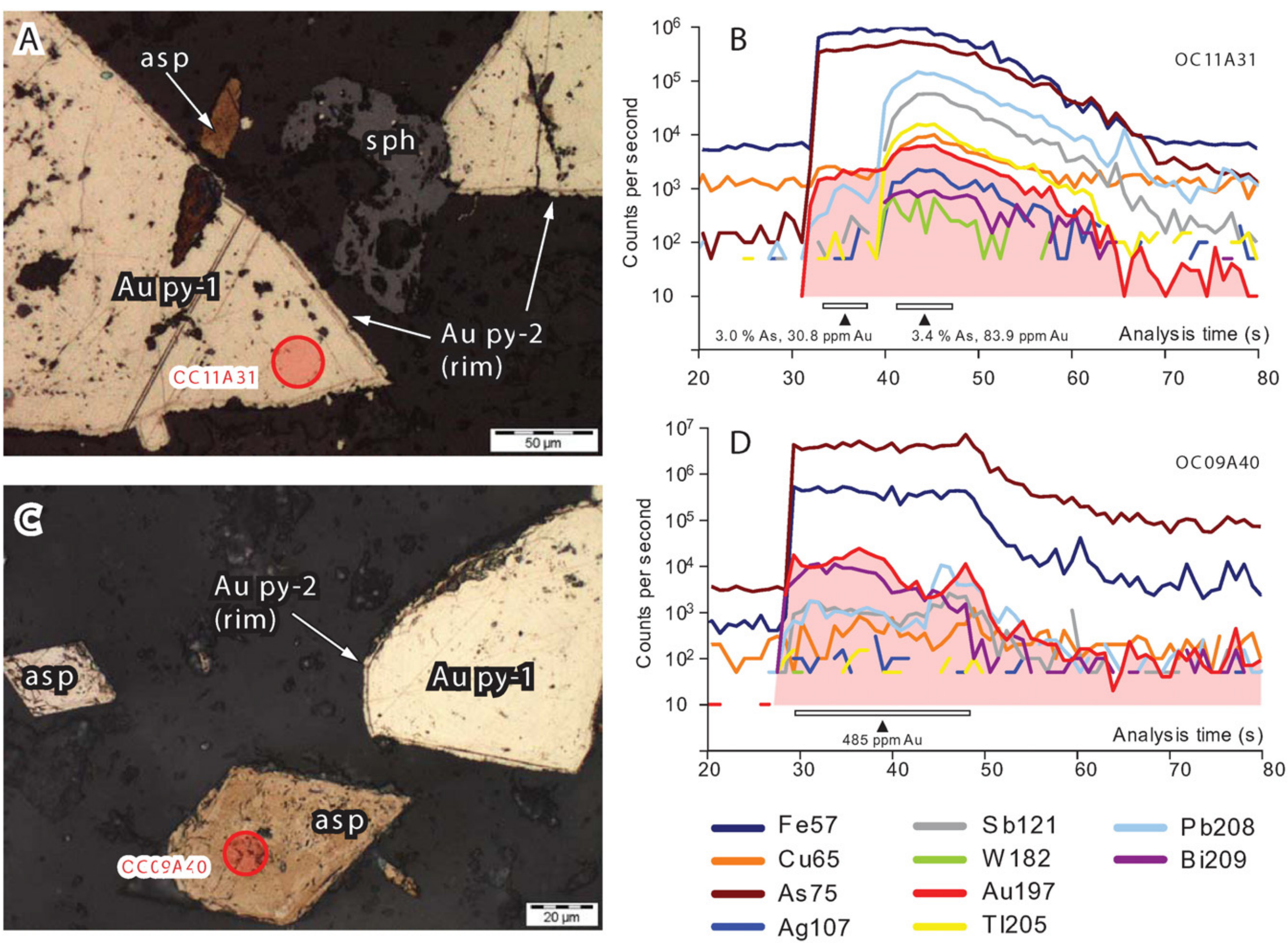


**Fig. 5.** Evidence for multi-stage gold mineralisation at the 20 Moz Gold Quarry deposit on the Carlin trend. A. Reflected light photomicrograph of relatively coarse-grained euhedral pyrite (*Au py-1*) and arsenopyrite (asp, tarnished brown due to $HNO_3$ etch) overgrown by a thin band of very fine-grained pyrite (*Au py-2*). Red spot shows the location of the LA–ICPMS analysis depicted in B. B. Plot of counts per second versus time for selected elements, during LA–ICPMS analysis of the pyrite grain depicted in A. The laser is turned on at ~30 s, and ablates through the grain and progressively into the surrounding matrix after 50 s. The abrupt increase in counts for Pb, Sb, Tl, Ag, Bi, W and Au (relative to Fe) after 40 s reflects an increasing contribution from the compositionally distinct *Au py-2* rimming the grain. This marked change in pyrite morphology and trace element composition suggests the two phases of auriferous pyrite precipitated under very different conditions, and possibly in different hydrothermal events. Both phases are interpreted to predate deposition of the more gold-rich (>800 ppm Au) Eocene Carlin-type pyrite at Gold Quarry. Sample is from the Deep Sulfide Feeder zone at Gold Quarry (drill hole QRC1750, 252′). C. Reflected light photomicrograph of arsenopyrite (tarnished brown due to $HNO_3$ etch) and pyrite in the same sample as A. Red spot shows the location of the LA–ICPMS analysis depicted in D. D. Plot of counts per second versus time for selected elements, during LA–ICPMS analysis of the arsenopyrite grain depicted in C. Arsenopyrite in this sample contains up to ca. 500 ppm Au, but low to very low levels of most other trace elements that are strongly enriched in Carlin-type pyrite.

Guinea) (Peterson and Mavrogenes, 2014) and giant Chuquicamata Cu deposit in Chile (Campbell et al., 2006). In the Porgera Au–Ag–Zn–Pb deposit, porphyry mineralisation was intersected by a fault system, which brought components from the host sediments and produced high grade Au–Te vein swarms (Sillitoe, 1994; Peterson and Mavrogenes, 2014). In many of porphyry deposits, the early stage gold is associated with Cu sulfides and electrum followed by the crystallization of late stage pyrite characterized by high As and gold inclusions (Gregory et al., 2013; Lang et al., 2013). Grasberg is another large porphyry deposits which show complex and protracted history with nested intrusions and hydrothermal alteration spanning a 1 Ma time period as evidenced by both Ar–Ar dating on mineralisation and intrusions (Pollard et al., 2005) and Re–Os geochronology on sulfides in ores (Mathur et al., 2005). The Cadia mineralised district in NSW, Australia also shows the presence of multiple porphyry mineralisation episodes clustering in tightly in space (0–5 km) but widely separated in time (18 Ma) (Wilson et al., 2007).

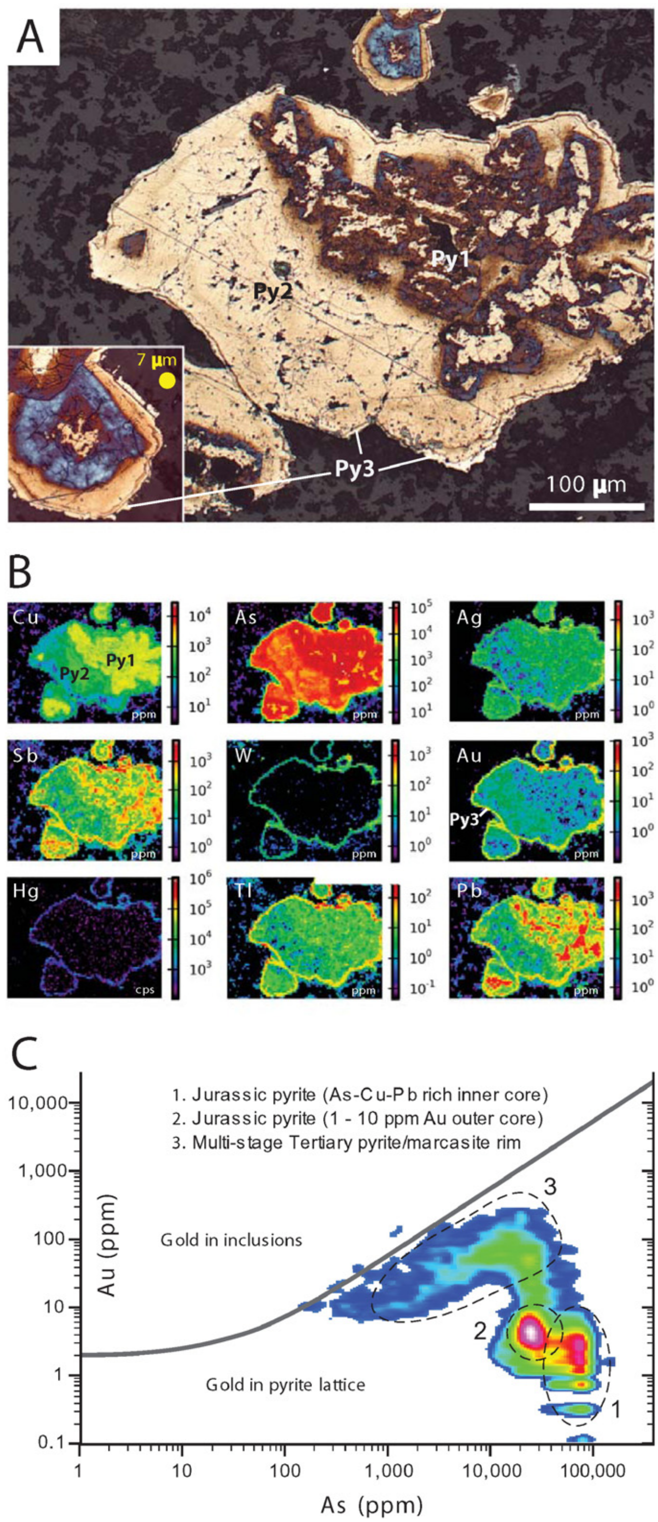


Fig. 6. Evidence for multi-stage gold mineralisation at the 7 Moz Meikle deposit on the north Carlin trend. A. Reflected light photomicrograph shows Jurassic pyrite (Py 1 tarnished by NaOCl etch) overgrown by multistage (Py2, Jurassic? to Tertiary) rims of very fine-grained pyrite and marcasite (see inset). The gold-rich Carlin-type pyrite forms an extremely narrow rim (3 Py barely perceptible, even in the inset) that coats both the Jurassic pyrite and a discontinuous fringe of fine grained marcasite (untarnished in inset). Host rock is a Jurassic monzonite dike (sample number EX92-904, see also Emsbo et al. (2003)). B. LA–ICPMS maps showing the distribution of selected trace elements for the pyrite grain depicted in A. Gold concentrations indicated for the 'rim' average up to 300 ppm Au, but are significantly less than the actual gold content of Carlin-type pyrite in this sample (1300–1600 ppm Au). As the Carlin-type pyrite rim is much narrower than the 7 μm laser spot size used for imaging (see inset in A). Accordingly, ppm concentrations for the 'rim' reflect mixtures of compositionally distinct pyrite types. The arsenic content of the zoned Jurassic pyrite (up to 10 wt.% As) is so high that that rim of Carlin-type pyrite (3–4 wt.% As, in this sample) is not apparent in the As map. Note that <1–13 ppm gold in the Jurassic pyrite shows a grossly antithetic relationship to As, Tl, Sb and Cu; elements with which gold is normally strongly correlated in Carlin-type pyrite. C. IoGAS contoured point density plot showing gold and arsenic concentrations for the pyrite depicted in A, superimposed on the gold solubility in pyrite plot of Reich et al. (2005). At least three discrete populations of auriferous pyrite are clearly apparent.

## 11. Discussion

Some of the concepts outlined in this paper are variations on a theme that has been extensively debated in the literature for over 100 years: namely; the source of the gold now found in the hydrothermal deposits (Knight, 1957; Meyer and Saager, 1985; Frimmel, 2008). Most recent studies accept that the source of metals will vary for different deposit types but there is currently no consensus for the majority of gold deposits worldwide and in particular the large deposits discussed here.

Although multi-stage gold enrichment processes are contentious for most of the deposits discussed above, this model deserves further examination because it could explain some of the major features of these deposits. From a practical point of view it would break down the huge enrichment factors required to make large, high grade gold ores into a series of smaller additive enrichment steps. Large enrichment factors are not impossible: for instance, engineers make these occur in mineral processing plants on a routine basis, but they require very efficient and sustained extraction. In ore deposits they also require the transport and deposition processes to occur and continue over a long time period, implying exceptional and rare events. A series of events overlapping in space could achieve the same outcome with smaller, less sustained and less efficient hydrothermal systems. Given the remarkable longevity of the continental crust on earth, we can expect that all hydrothermal systems will one day be either reworked by magmatism, metamorphism or erosion. These processes can disperse the gold but can also add to the original enrichment by further concentrating the gold or adding to the original gold inventory.

There are a number of possible ways in which a multi-stage model might work:

1. Upgrading of an early lower grade source rock (e.g. carbonaceous shale or pyritic volcaniclastic rocks) to a high grade deposit by late stage magmatic, structural or metamorphic processes. For example, a low grade regional upper crustal or mid-crustal gold source rock at the 0.1 ppm Au level needs to only undergo a 10 to 100 fold concentration process to make ore grade (1–10 ppm Au) compared to the 1000–10,000 enrichment factor required for normal background

igneous or sedimentary rocks (0.001–0.01 ppm; Tomkins, 2013) (0.001–0.01 ppm; Tomkins, 2013). Large enrichment factors are possible but less probable (i.e. require a more exceptional set of circumstances) than a series of smaller enrichments.

2. Reactivation of structures during deformation or magmatic events causing pulses of gold-bearing fluid to migrate along a single pathway.
3. Early hydrothermal or syngenetic mineralization acting as a chemical trap (e.g. redox) for subsequent epigenetic mineralization.
4. Multiple intrusions causing multiple hydrothermal systems either reworking the earlier gold enrichment events or adding to the metal budgets.

Multi-stage gold enrichment models will necessarily be more complex than those involving a single stage. The possibility of multiple sources, transport pathways and traps operating at various times in the deposit's geological history could explain the observations from many studies of gold deposits that show overprinting vein relationships and overlapping alteration zones (e.g. Buchholz et al., 2007; Cabral et al., 2011; Thomas et al., 2011; Simard et al., 2013). In many previous studies this complexity is ascribed to changes in the physical and/or chemical condition within a short (<1 Ma) time period, as the hydrothermal fluids invade the area, reach peak temperature and then cool to ambient conditions. However, in some deposits these events are likely to have occurred a number of times, particularly with some of the older deposits in Paleozoic and Precambrian fold belts that have been involved in multiple orogenic events or in subduction-related environments which have been affected by multiple magmatic pulses.

Various studies hypothesize that gold mineralization is associated with major crustal scale structures in areas that have undergone large scale gold enrichment or fertilization of the lower crust or the upper mantle (Groves, 1993; Phillips and Powell, 2010; Hronsky et al., 2012) leading to gold provinces or camps that contain numerous deposits. If that is the case, then it follows that these structures and sources should be able to provide fresh gold-bearing fluids to discrete sites during more than one orogenic, structural or magmatic event. This could not only produce some of the complex vein and ore relationships that typify many gold deposits but also provide multiple sources of gold that could be reworked again by later orogenesis, erosion, magmatism or hydrothermal fluids. Multi-stage deposit formation should also occur when the gold endowment or enrichment is related to shallower sedimentary processes with gold enriched in a low-grade sedimentary sequence in a deep basin being reworked by later processes (Pitcairn et al., 2006; Large et al., 2011; Tomkins, 2013). In the telescoped porphyry/epithermal mineralization, the early ore minerals tend to interact strongly with later mineralisation. In the nested porphyries such as Grasberg and Cadia the interaction between the early and late events are cryptic.

- The early mineralisation could have been partially reworked by latter events.
- The area's geology and magma types are predisposed to gold mineralisation but there are no other interactions between the events.
- The proximity of the multiple systems is simply a coincidence.

All three of these possibilities will lead to the formation of larger deposits than if a single event was present. The first two possibilities are likely to occur in concert so that if an area has the right ingredients for mineralisation, then the chance of the early gold being reworked are high leading to large clustered multistage mineralisation. This style of mineralisation is will also be favored in magmatic systems that experience prolonged evolution for millions of years with episodic flare ups in magmatic activity (Ducea et al., 2015). It could be argued that the multiple events that have been documented in the larger gold deposits occur because they tend to better studied. However, logically it must follow that having two mineral systems in close proximity must generally increase the tonnage irrespective of a literature bias.

One of the major problems with many gold deposits is that precise geochronological constraints on mineralization are difficult to establish. Direct dating of gold minerals is difficult, and most studies rely on evidence for co-precipitation with high K, Pb, U, Rb, Sm or Re minerals which can be dated with isotopic determinations or indirect evidence, either from the age of the host rock or from cross-cutting relationships from late magmatic events. Another problem is that where early hydrothermal processes are overprinted by later events, the evidence for early enrichment is commonly obliterated. Even when multiple hydrothermal ages are obtained for a deposit, it is very difficult to provide estimates of the amount of gold concentrated within each of the events. For example, in most deposits which show multiple hydrothermal pulses, it is extremely difficult to provide accurate quantification of the relative importance of the meter-scale remobilization of early gold versus fresh input of new gold on the kilometer scale. Most of the estimates that can be formulated are model dependent and rely on a handful of geochronology data which are biased towards the occurrence of a datable mineral. Accurate estimates would require hundreds to thousands of data measurements similar to that typically used for resource estimates. In this study we have compiled geochronological data for the various gold mineralisation stages on the deposits discussed in detail and presented some rudimentary estimate on the importance of each events (Appendix 1).

One of the techniques that has been used to document successive pulses of gold enrichment is mapping of the distribution of trace elements in pyrite and measurements of Pb isotopes (Large et al., 2009). The $H_2S$-bearing fluids are able to transport gold in sulfide complexes (Phillips and Powell, 2010; Tomkins, 2010) tend to promote the growth of pyrite during gold mineralization. Pyrite can readily incorporate both gold and lead in its lattice, providing both a record of gold abundance and a chronometer within its crystal structure (Meffre et al., 2008). Unfortunately in most cases the common Pb incorporated within the pyrite provides imprecise Pb growth model ages which are capable of distinguishing gold mineralization events tens of millions of years apart at least. In many gold deposits this has been sufficient to show the presences of multiple gold events (e.g. Witwatersrand, Sukhoi Log, Bendigo; Meffre et al., 2008; Thomas et al., 2011; Large et al., 2013). In other areas (e.g., Kalgoorlie) the gold deposition processes may be too close in time to be resolved using the Pb isotope technique. In some deposits, such as Carlin, the heterogeneity of the Pb in the fluid source regions is too complex to be unraveled using these techniques (Tosdal et al., 2003). Another technique that holds promise in unraveling the history of individual crystals that have complex growth zones is Re–Os geochronology. However, although it has been shown to be reliable in dating some pyrite, chalcopyrite and arsenopyrite, at present it does not have the spatial resolution to be able to date minerals with multiple growth zones.

These techniques have to date only been applied to a small number of deposits worldwide and have shown in recent years that many of the largest deposits have complex gold sources and enrichment histories. With continued forensic research of this type it is possible that the presence of multiple gold enrichment processes will be discovered at many of the large deposits across the world. On the basis of the deposits examined here we would argue that the largest gold deposits worldwide have protracted gold enrichment histories that involve multiple gold sources and that the presence of these multiple gold events can be used as an indicator of fertility and size. Thus deposits showing complex paragenesis, and minerals recording multiple gold events, could be considered more attractive exploration targets that those with simple hydrothermal histories.

## 12. Conclusion

A growing number of giant gold deposits have been demonstrated to form in multi-stage processes that occur over millions or even billions of years. From a theoretical and logical point of view, a multi-stage origin mechanism is attractive because it involves coincident small steps that overlap in space (but generally not time) to create large high-grade accumulations of gold. However, it also has practical applications for gold exploration worldwide. For example, the coincidence of a low grade syngenetic gold halo within a rock unit with a late stage structure (i.e. fault, anticline or unconformity) could be an attractive exploration target. From an ore genesis point of view, this concept has the potential to merge much of the syngenetic versus epigenetic debate, which has polarized geologic opinions worldwide, into a coherent framework, in which many of these deposits have both syngenetic and epigenetic stages. In the porphyry environment, areas containing multiple small intrusions with complex sulfide paragenesis could be prioritized over areas with simpler magmatic histories and/or containing simpler sulfide paragenesis or geochronology. Of course, given the diversity and complexity of gold ore deposits worldwide, this mechanism will not be applicable for all gold deposits and any appeals to a multi-stage history must be based on firm geological evidence. Large super-efficient, long-lived hydrothermal systems are likely to have operated in some instances and therefore this type of process must be responsible for at least some of the large deposits worldwide. Fortunately new micro-analytical techniques developed over the last 20 years make millimeter scale images of the distribution of gold and other elements associated with mineralization easier to obtain, leading to an increasingly sophisticated understanding of the ore genesis process.

## Acknowledgments

The sponsors of AMIRA P1041 (AngloGold Ashanti, Newcrest, Newmont, G3, Issara and Sipa Resources) are thanked for supporting the original research into laser ablation mass spectrometry and gold mineralisation. BHP Billiton and ARC linkage grant (LP130100438) to Kamenetsky, Meffre and Ehrig also helped support this research. Daniel Gregory thanks John Walsh, Adam Bath and Goldfields. Thanks to David Huston and an anonymous reviewer for excellent constructive reviews that significantly improved the manuscript.

## Appendix A. Appendix 1 Table

| Deposit | Style | Age (Ma) | Temporal constraints | Mineral | Significance of event | Reference |
|---|---|---|---|---|---|---|
| *Sukhoi log* | | | | | | |
| Early | Disceminated pyrite | 573 ± 13 | U–Pb | Monazite | | Meffre et al. 2008 |
| Intermediate | Orogenic vein | 505 ± 19* | Re–Os | Pyrite | Major | Yakubchuk et al. 2014 |
| Intermediate | Orogenic vein | 516 ± 10 | U–Pb | Monazite | Major | Meffre et al. 2008 |
| Late | Minor reworking | 314 ± 20, 288 ± 22 | U–Pb | Monazite | Minor | Meffre et al. 2008 |
| *Olympiada* | | | | | | |
| Early | Heterogeneity in Re | ? | Re–Os | Pyrite | Minor | Yakubchuk et al. 2014 |
| Late | Orogenic vein | 511 ± 24* | Re–Os | Pyrite | Major | Yakubchuk et al. 2014 |
| *Witwatersrand* | | | | | | |
| Early | Detrital | 3100–2800 | Model Pb | Pyrite | Major-moderate | Barton and Hallbauer, 1996; Poujol et al., 1999; Large et al., 2013 |
| Early | Detrital | 3030 ± 21* | Re–Os | Gold and pyrite | Major | Kirk et al., 2001 |
| Early | Detrital | 3090 ± 2 to 2798 ± 14 | U–Pb | Xenotime | Major | Kositcin et al., 2003 |
| Intermediate | | 2121 ± 9 | U–Pb | Monazite | Minor | Rasmussen et al., 2007 |
| Late | Pyrite overgrowth | 2032 ± 5* | U–Pb | Monazite | Uncertain | Rasmussen et al., 2007 |
| Late | Pyrite overgrowth | 2069 ± 48 Ma | Pb–Pb isochron | Pyrite with U inclusions | Moderate | Large et al., 2013 |
| Late | Pyrite overgrowth | 2050 | Re–Os | Pyrite | Moderate | Mathur et al., 2013 |
| *Grasberg* | | | | | | |
| Early | Porphyry | 3.41 ± 0.03 | Ar–Ar | Phlogopite | Minor | Pollard et al., 2005 |
| Intermediate | Porphyry | 3.33 ± 0.12 to 3.01 ± 0.06 | Ar–Ar | K-feldspar and biotite | Major | Pollard et al., 2005 |
| Late | Porphyry | 2.59 ± 0.15 | Ar–Ar | Phlogopite | Minor | Pollard et al., 2005 |
| *Pebble* | | | | | | |
| Early | Porphyry | 90.4 ± 0.6 to 89.5 ± 0.3 | Re–Os | Molybdenite | Major | Lang et al., 2013 |
| Early | Porphyry | 88.5 ± 0.3 | Ar–Ar | Biotite | Major | Lang et al., 2013 |
| Intermediate | Porphyry | 86.0 ± 0.2 | Ar–Ar | K-feldspar | Minor | Lang et al., 2013 |
| Late | Porphyry | 46.1 ± 0.2 | Ar–Ar | K-feldspar | Minor | Lang et al., 2013 |
| Cadia | | | | | | |
| Early | Porphyry | 459.7 ± 1.4 to 450.5 ± 1.7 | Re–Os | Molybdenite | Major | Wilson et al., 2007 |
| Late | Porphyry | 443.5 ± 1.4 to 435.9 ± 3.7 | Re–Os | Molybdenite | Major | Wilson et al., 2007 |
| *Bendigo* | | | | | | |
| Early | Disceminated pyrite | After 470 Ma | Textural interpretation | Pyrite | Pre-concentration | Thomas et al., 2011 |
| Late | Orogenic saddle reefs | 443 + 3 | Ar–Ar | Sericite | Major | Phillips et al., 2012 |
| Late | Orogenic saddle reefs | 438 + 6 | Re–Os | Arsenopyrite and pyrite | Major | Phillips et al., 2012 |
| *Carlin* | | | | | | |
| Early | Sedex | Late Devonian | Textural/host rock age | Gold and pyrite | Major | Emsbo et al., 1999, 2003, 2006 |
| Intermediate | Intrusion-related polymetallic mineralization | 154.6 ± 1.4 | Ar–Ar | Sericite | Moderate | Emsbo et al., 2000 |
| Late | Carlin-type | 42 to 33 | Rb/Sr, U/Th–He, K–Ar, Ar–Ar, U–Pb | Galkhaite, apatite, biotite, plagioclase, zircon | Major | Arehart et al., 2003 |

**Appendix** (*continued*)

| Deposit | Style | Age (Ma) | Temporal constraints | Mineral | Significance of event | Reference |
|---|---|---|---|---|---|---|
| *St. Ives* | | | | | | |
| Host age | | 2692 ± 4 Ma | U–Pb | Zircon | | Claoue-Long et al., 1988 |
| Early | Diagenetic/syngenitic Pyrite nodule and disseminations | | Textural interpretation | Pyrite | Minor | Gregory, 2014 |
| Late | Gold bearing shear zones (at Mt. Charlotte, 60 km to north) | 2655 ± 4 Ma | U–Pb | Xenotime | Major | Rasmussen et al., 2009 |
| Late | Gold bearing shear zones | 2630 Ma | U–Pb | Monazite | Major | Nguyen, 1997 |
| *Kalgoorlie* | | | | | | |
| Host age | | 2680 ± 9 Ma | U–Pb | Zircon | | Rasmussen et al., 2009 |
| Early | Diagenetic/syngenitic pyrite nodule and disseminations | | Textural interpretation | Pyrite | Minor | Steadman et al., 2014 |
| Intermediate | Oroya Style ore | 2642 ± 6 | U–Pb | Zircon in syn gold dyke | Major | Vielreicher et al., 2015 |
| Late | Shea West | 2611 ± 9 Ma | Re–Os | Molybdenite | Minor | Vielreicher et al., 2010 |
| Late | Veins in Mt Charlotte and Fimiston ores | 2610 ± 4 to 2617 ± 12 | Ar–Ar | Sericite in ores | Minor | Heath 2003 in Vielreicher et al., 2015 |
| *Boddington* | | | | | | |
| Early | Porphyry | 2707 ± 17 | Re–Os | Molybdenite | Minor | Ciobanu et al., 2013b |
| Late | Intrusion-related | 2623 ± 9 | Re–Os | Molybdenite | Major | Ciobanu et al., 2013b |
| Lihir | | | | | | |
| Early | Porphyry | 0.91 ± 0.10 to 0.336 ± 0.027 | K–Ar | Biotite | Minor | Reviewed by Blackwell, 2010 |
| Intermediate | Epithermal | 0.61 ± 0.25 to 0.52 ± 0.11 | Ar–Ar | Adularia | Major | Blackwell et al., 2014 |
| Late | Clay | 0.151 ± 0.015 Ma | K–Ar | Clay | Minor | Reviewed by Blackwell, 2010 |
| *Olympic Dam* | | | | | | |
| Early | IOCG | 1590 ± 8 Ma and 1577 ± 5 | Pb–Pb | Hematite | Major | Ciobanu et al., 2013b |
| Intermediate | IOCG | 1400 to 1100 | Pb–Pb, Rb–Sr, Nd–Sm | Ores | Major | Maas et al., 2011 |
| Intermediate | IOCG | 1258 + 28 | Re–Os | Chalcopyrite and pyrite | Minor | McInnes et al., 2008 |
| Late | Structurally controlled | 450 to 550 | Rb–Sr | Sericite and fluorite | Minor | Maas et al., 2011 |

* = Most precise age of a number of ages.

## References


Agangi, A., Hofmann, A., Rollion-Bard, C., Marin-Carbonne, J., Cavalazzi, B., Large, R., Meffre, S., 2015. Gold accumulation in the Archaean Witwatersrand basin, South Africa-evidence from concentrically laminated pyrite. Earth Sci. Rev. 140, 27–53.

Allibone, A.H., Windh, J., Etheridge, M.A., Burton, D., Anderson, G., Edwards, P.W., Miller, A., Graves, C., Fanning, C.M., Wysoczanski, R., 1998. Timing relationships and structural controls on the location of Au–Cu mineralization at the Boddington gold mine, Western Australia. Econ. Geol. 93, 245–270.

Arehart, G.B., Chakurian, A.M., Tretbar, D.R., Christensen, J.N., McInnes, B.A., Donelick, R.A., 2003. Evaluation of radioisotope dating of Carlin-type deposits in the Great Basin, Western North America, and implications for deposit genesis. Econ. Geol. 98, 235–248.

Barker, S.L.L., Hickey, K.A., Cline, J.S., Dipple, G.M., Kilburn, M.R., Vaughan, J.R., Longo, A.A., 2009. Uncloaking invisible gold: use of NanoSIMS to evaluate gold, trace elements, and sulfur isotopes in pyrite from Carlin-type gold deposits. Econ. Geol. 104, 897–904.

Barton, E.S., Hallbauer, D.K., 1996. Trace-element and U–Pb isotope compositions of pyrite types in the Proterozoic black reef, Transvaal sequence, South Africa: implications on genesis and age. Chem. Geol. 133, 173–199.

Bateman, R., Hagemann, S., 2004. Gold mineralisation throughout about 45 Ma of Archaean orogenesis: protracted flux of gold in the Golden Mile, Yilgarn craton, Western Australia. Mineral. Deposita 39, 536–559.

Bath, A.B., Walshe, J.L., Cloutier, J., Verrall, M., Cleverley, J.S., Pownceby, M.I., Macrae, C.M., Wilson, N.C., Tunjic, J., Nortje, G.S., et al., 2013. Biotite and apatite as tools for tracking pathways of oxidized fluids in the Archean east repulse gold deposit, Australia. Econ. Geol. 108, 667–690.

Blackwell, J.L., 2010. Lithofacies Associations and Evolution of the Volcanic Host Succession to the Minifie ore Zone: Ladolam Gold Deposit. University of Tamania, Lihir Island, Papua New Guinea.

Blackwell, J.L., Cooke, D.R., McPhie, J., Simpson, K.A., 2014. Lithofacies associations and evolution of the volcanic host succession to the minifie ore zone: ladolam gold deposit, lihir Island, Papua New Guinea. Econ. Geol. 109, 1137–1160.

Blewett, R.S., Squire, R., Miller, J.M., Henson, P.A., Champion, D.C., 2010. Architecture and geodynamic evolution of the St Ives goldfield, eastern Yilgarn Craton, Western Australia. Precambrian Res. 183, 275–291.

Buchholz, P., Oberthür, T., Lüders, V., Wilkinson, J., 2007. Multistage Au–As–Sb mineralization and crustal-scale fluid evolution in the Kwekwe district, Midlands Greenstone Belt, Zimbabwe: a combined geochemical, mineralogical, stable isotope, and fluid inclusion study. Econ. Geol. 102, 347–378.

Cabral, A.R., Burgess, R., Lehmann, B., 2011. Late Cretaceous bonanza-style metal enrichment in the Serra Pelada Au–Pd–Pt deposit, Pará, Brazil. Econ. Geol. 106, 119–125.

Campbell, I.H., Ballard, J.R., Palin, J.M., Allen, C., Faunes, A., 2006. U–Pb zircon geochronology of granitic rocks from the Chuquicamata-El Abra porphyry copper belt of northern Chile: excimer laser ablation ICP-MS analysis. Econ. Geol. 101, 1327–1344.

Ciobanu, C.L., Cook, N.J., Kelson, C.R., Guerin, R., Kalleske, N., Danyushevsky, L., 2013a. Trace element heterogeneity in molybdenite fingerprints stages of mineralization. Chem. Geol. 347, 175–189.

Ciobanu, C.L., Wade, B.P., Cook, N.J., Schmidt, M.A., Giles, D., 2013b. Uranium-bearing hematite from the Olympic Dam Cu–U–Au deposit, South Australia: a geochemical tracer and reconnaissance Pb–Pb geochronometer. Precambrian Res. 238, 129–147.

Claoue-Long, J.C., Compston, W., Cowden, A., 1988. The age of the Kambalda greenstones resolved by ion-microprobe: implications for Archaean dating methods. Earth Planet. Sci. Lett. 89, 239–259.

Cline, J.S., Hofstra, A.H., Muntean, J.L., Tosdal, R.M., Hickey, K.A., 2005. Carlin-Type Gold Deposits in Nevada; Critical Geologic Characteristics and Viable Models. In: Hedenquist, J.W., Thompson, J.F.H., Goldfarb, R.J., Richards, J.P. (Eds.), Economic Geology; one Hundredth Anniversary vol. 1905–2005. Society of Economic Geologists, Littleton, CO, United States, pp. 451–484.

Clout, J.M.F., 1989. Structural and Isotopic Studies of the Golden Mile Gold-Telluride Deposit, Kalgoorlie, WA [PhD] Monash University, Melbourne.

Clout, J.M.F., Cleghorn, J.H., Eaton, P.C., 1990. Geology of the Kalgoorlie gold field. Monograph Series — Australasian Institute of Mining and Metallurgy 14, pp. 411–431.

Crafford, A.E.J., Grauch, V.J.S., 2002. Geologic and geophysical evidence for the influence of deep crustal structures on Paleozoic tectonics and the alignment of world-class gold deposits, north-central Nevada, USA. Ore Geol. Rev. 21, 157–184.

Ducea, M.N., Paterson, S.R., DeCelles, P.G., 2015. High-volume magmatic events in subduction systems. Elements. 11, 99–104.

Emsbo, P., Hutchinson, R.W., Hofstra, A.H., Volk, J.A., Bettles, K.H., Baschuk, G.J., Johnson, C.A., 1999. Syngenetic Au on the Carlin trend: implications for Carlin-type deposits. Geology 27, 59–62.

Emsbo P., Hofstra A.H., Lauha E.A., 2000. Jurassic Auriferous Polymetallic Mineralization at the Goldstrike Mine, Carlin Trend, Nevada. In: Cluer J., Price J., Struhsacker E., Hardyman R., Morris L., Editors. Geology and Ore Deposits 2000: The Great Basin and Beyond. Symposium proceedings. Reno: Geological Society of Nevada, pp. 46.

Emsbo, P., Hofstra, A.H., Lauha, E.A., Griffin, G.L., Hutchinson, R.W., 2003. Origin of high-grade gold ore, source of ore fluid components, and genesis of the Meikle and neighboring Carlin-type deposits, northern Carlin trend, Nevada. Econ. Geol. 98, 1069–1100.

Emsbo, P., Groves, D., Hofstra, A., Bierlein, F., 2006. The giant Carlin gold province: a protracted interplay of orogenic, basinal, and hydrothermal processes above a lithospheric boundary. Mineral. Deposita 41, 517–525.

England, G.L., Rasmussen, B., McNaughton, N.J., Fletcher, I.R., Groves, D.I., Krapez, B., 2001. SHRIMP U–Pb ages of diagenetic and hydrothermal xenotime from the Archaean Witwatersrand supergroup of South Africa. Terra Nova 13, 360–367.

Frimmel, H.E., 2008. Earth's continental crustal gold endowment. Earth Planet Sci. Lett. 267, 45–55.

Gregory, D.D., 2014. The Trace Element Composition of Sedimentary Pyrite: Factors Effecting Uptake and Uses of the Data for Determining Paleo-Ocean Conditions [PhD] University of Tasmania, Hobart, Tasmania.

Gregory, M.J., Lang, J.R., Gilbert, S., Hoal, K.O., 2013. Geometallurgy of the pebble porphyry copper–gold–molybdenum deposit, Alaska: implications for gold distribution and paragenesis. Econ. Geol. 108, 463–482.
Gregory, D., Meffre, S., Large, R., 2014. Comparison of metal enrichment in pyrite framboids from a metal-enriched and metal-poor estuary. Am. Mineral. 99, 633–644.
Groves, D.I., 1993. The crustal continuum model for late-Archaean lode-gold deposits of the Yilgarn Block, Western Australia. Mineral. Deposita 28, 366–374.
Hronsky, J.M.A., Groves, D.I., Loucks, R.R., Begg, G.C., 2012. A unified model for gold mineralisation in accretionary orogens and implications for regional-scale exploration targeting methods. Mineral. Deposita 47, 339–358.
Huang, Q., Kamenetsky, V., Mcphie, J., Ehrig, K., Meffre, S., Maas, R., Apukhtina, O., Kamenetsky, M., Chambefor, I., 2015. Enter title. Precambrian Res. (in press).
Kirk, J., Ruiz, J., Chesley, J., Titley, S., Walshe, J., 2001. A detrital model for the origin of gold and sulfides in the Witwatersrand basin based on Re–Os isotopes. Geochim. Cosmochim. Acta. 65, 2149–2159.
Knight, C.L., 1957. Ore genesis—the source bed concept. Econ. Geol. 52, 808–817.
Kositcin, N., McNaughton, N.J., Griffin, B.J., Fletcher, I.R., Groves, D.I., Rasmussen, B., 2003. Textural and geochemical discrimination between xenotime of different origin in the Archaean Witwatersrand basin, South Africa. Geochim. Cosmochim. Acta. 67, 709–731.
Lang, J.R., Gregory, M.J., Rebagliati, C.M., Payne, J.G., Oliver, J.L., Roberts, K., 2013. Geology and magmatic-hydrothermal evolution of the giant pebble porphyry copper–gold–molybdenum deposit, southwest Alaska. Econ. Geol. 108, 437–462.
Large, R.R., Maslennikov, V.V., Robert, F., Danyushevsky, L.V., Chang, Z., 2007a. Multistage sedimentary and metamorphic origin of pyrite and gold in the giant Sukhoi log deposit, Lena Gold Province, Russia. Econ. Geol. 102, 1233–1267.
Large, R.R., Maslennikov, V.V., Robert, F., Danyushevsky, L.V., Chang, Z.S., 2007b. Multistage sedimentary and metamorphic origin of pyrite and gold in the giant Sukhoi log deposit, Lena Gold province, Russia. Econ. Geol. 102, 1233–1267.
Large, R.R., Danyushevsky, L., Hollit, C., Maslennikov, V., Meffre, S., Gilbert, S., Bull, S., Scott, R., Emsbo, P., Thomas, H., et al., 2009. Gold and trace element zonation in pyrite using a laser imaging technique: implications for the timing of gold in orogenic and Carlin-style sediment-hosted deposits. Econ. Geol. 104, 635–668.
Large, R.R., Bull, S.W., Maslennikov, V.V., 2011. A carbonaceous sedimentary source-rock model for Carlin-type and orogenic gold deposits. Econ. Geol. 106, 331–358.
Large, R.R., Meffre, S., Burnett, R., Guy, B., Bull, S., Gilbert, S., Goemann, K., Danyushevsky, L., 2013. Evidence for an intrabasinal source and multiple concentration processes in the formation of the carbon leader reef, Witwatersrand supergroup, South Africa. Econ. Geol. 108, 1215–1241.
Large, R.R., Halpin, J.A., Danyushevsky, L.V., Maslennikov, V.V., Bull, S.W., Long, J.A., Gregory, D.D., Lounejeva, E., Lyons, T.W., Sack, P.J., et al., 2014. Trace element content of sedimentary pyrite as a new proxy for deep-time ocean–atmosphere evolution. Earth Planet Sci. Lett. 389, 209–220.
Large, R.R., Gregory, D.D., Steadman, J.A., Tomkins, A.G., Lounejeva, E., Danyushevsky, L.V., Halpin, J.A., Maslennikov, V., Sack, P.J., Mukherjee, I., et al., 2015. Gold in the oceans through time. Earth Planet Sci. Lett. 428, 139–150.
Law, J., Phillips, N., 2006. Witwatersrand gold-pyrite-uraninite deposits do not support a reducing Archean atmosphere. Mem. Geol. Soc. Am. 121–141.
Laznicka, P., 2014. Giant metallic deposits—a century of progress. Ore Geol. Rev. 62, 259–314.
Maas, R., Kamenetsky, V., Ehrig, K., Meffre, S., McPhie, J., Diemar, G., 2011. Olympic Dam U–Cu–Au deposit, Australia; new age constraints. Mineral. Mag. 75, 1375.
Mathur, R., Gauert, C., Ruiz, J., Linton, P., 2013. Evidence for mixing of Re–Os isotopes at <2.7 Ga and support of a remobilized placer model in Witwatersrand sulfides and native Au. Lithos 164-167, 65–73.
Mathur, R., Titley, S., Ruiz, J., Gibbins, S., Friehauf, K., 2005. A Re–Os isotope study of sedimentary rocks and copper-gold ores from the Ertsberg district, west Papua, Indonesia. Ore Geol. Rev. 26, 207–226.
McCuaig, T.C., Behn, M., Stein, H.J., Hagemann, S.G., McNaughton, N.J., Cassidy, K.F., Champion, D.C., Wyborn, L., 2001. The Boddington gold mine; a new style of Archaean Au–Cu deposit. Record – Australian Geological Survey Organisation, pp. 453–455.
McInnes, B.I.A., Keays, R.R., Lambert, D.D., Hellstrom, J., Allwood, J.S., 2008. Re–Os geochronology and isotope systematics of the Tanami, Tennant Creek and Olympic Dam Cu–Au deposits. Aust. J. Earth Sci. 55, 967–981.
McNaughton, N.J., Mueller, A.G., Groves, D.I., 2005. The age of the giant golden mile deposit, Kalgoorlie, Western Australia: ion-microprobe zircon and monazite U–Pb geochronology of a synmineralization lamprophyre dike. Econ. Geol. 100, 1427–1440.
McPhie, J., Kamenetsky, V., Allen, S., Ehrig, K., Agangi, A., Bath, A., 2011a. The fluorine link between a supergiant ore deposit and a silicic large igneous province. Geology 39, 1003–1006.
McPhie, J., Kamenetsky, V.S., Chambefort, I., Ehrig, K., Green, N., 2011b. Origin of the supergiant Olympic Dam Cu–U–Au–Ag deposit, South Australia: was a sedimentary basin involved. Geology 39, 795–798.
Meffre S., Kamenetsky V., McPhie J., Maas R., Ehrig K., Chambefort I., 2010. Pb isotopes at Olympic Dam: constraining sulphide growth. 13th Quadrennial IAGOD Symposium; Giant Ore Deposits Down-Under. Adelaidepp. 78–79.
Meffre, S., Large, R.R., Scott, R., Woodhead, J., Chang, Z., Gilbert, S.E., Danyushevsky, L.V., Maslennikov, V., Hergt, J.M., 2008. Age and pyrite Pb-isotopic composition of the giant Sukhoi log sediment-hosted gold deposit, Russia. Geochim. Cosmochim. Acta 72, 2377–2391.
Meyer, M., Saager, R., 1985. The gold content of some Archaean rocks and their possible relationship to epigenetic gold–quartz vein deposits. Mineral. Deposita 20, 284–289.
Miller, J., Blewett, R., Tunjic, J., Connors, K., 2010. The role of early formed structures on the development of the world class St Ives goldfield, Yilgarn, WA. Precambrian Res. 183, 292–315.
Minter, W.E.L., 1999. Irrefutable detrital origin of Witwatersrand gold and evidence of eolian signatures. Econ. Geol. 94, 665–670.
Neumayr, P., Walshe, J., Hagemann, S., Petersen, K., Roache, A., Frikken, P., Horn, L., Halley, S., 2008. Oxidized and reduced mineral assemblages in greenstone belt rocks of the St. Ives gold camp, Western Australia: vectors to high-grade ore bodies in Archaean gold deposits? Mineral. Deposita 43, 363–371.
Nguyen, T., 1997. Structural Controls on Gold Mineralisation of the Revenge Deposit and Its Setting in the Lake Lefroy Area. The University of Western Australia, Kambalda, Western Australia.
Nichols, S.J., Hagemann, S.G., 2014. Structural and hydrothermal alteration evidence for two gold mineralisation events at the new celebration gold deposits in Western Australia. Aust. J. Earth Sci. 61, 113–141.
Nickel, E.H., 1977. Mineralogy of the "green leader" gold ore at Kalgoorlie, Western Australia. Proc. Australas. Inst. Mineral. Metall. 263, 9–13.
Nixon, D.G., Hesford, C., Fitzgerald, M., Lister, G., 2014. Relative Timing of Gold Mineralisation within the Kalgoorlie Camp. Gold14@Kalgoorlie — International Symposium. Curtin University, KalgoorlieAustralian Institute of Geoscientists, Australia, pp. 97–98.
Nutt, C.J., Hofstra, A.H., 2007. Bald mountain gold mining district, Nevada: a Jurassic reduced intrusion-related gold system. Econ. Geol. 102, 1129–1155.
Oberthür, T., Weiser, T., Amanor, J.A., Chryssoulis, S.L., 1997. Mineralogical siting and distribution of gold in quartz veins and sulfide ores of the Ashanti mine and other deposits in the Ashanti belt of Ghana: genetic implications. Mineral. Deposita 32, 2–15.
Peterson, E.C., Mavrogenes, J.A., 2014. Linking high-grade gold mineralization to earthquake-induced faultvalve processes in the Porgera gold deposit, Papua New Guinea. Geology 42, 383–386.
Phillips, D., Fu, B., Wilson, C.J.L., Kendrick, M.A., Fairmaid, A.M., Miller, J.M., 2012. Timing of gold mineralisation in the western Lachlan orogen, SE Australia: a critical overview. Aust. J. Earth Sci. 59, 495–525.
Phillips, G.N., 1986. Geology and alteration in the golden mile, Kalgoorlie. Econ. Geol. 81, 779–808.
Phillips, G.N., Powell, R., 2010. Formation of gold deposits: a metamorphic devolatilization model. J. Metamorph. Geol. 28, 689–718.
Phillips, G.N., Powell, R., 2015. Hydrothermal alteration in the Witwatersrand goldfields. Ore Geol. Rev. 65, 245–273 (Part 1).
Pitcairn, I.K., Teagle, D.A.H., Craw, D., Olivo, G.R., Kerrich, R., Brewer, T.S., 2006. Sources of metals and fluids in orogenic gold deposits: insights from the Otago and alpine schists, New Zealand. Econ. Geol. 101, 1525–1546.
Pollard, P.J., Taylor, R.G., Peters, L., 2005. Ages of intrusion, alteration and mineralization at the Grasberg Cu–Au deposit, Papua, Indonesia. Econ. Geol. 100, 1005–1020.
Poujol, M., Robb, L.J., Respaut, J.P., 1999. U–Pb and Pb–Pb isotopic studies relating to the origin of gold mineralization in the Evander Goldfield, Witwatersrand Basin, South Africa. Precambrian Res. 95, 167–185.
Rasmussen, B., Fletcher, I.R., Muhling, J.R., Mueller, A.G., Hall, G.C., 2007. Bushveld-aged fluid flow, peak metamorphism, and gold mobilization in the Witwatersrand basin, South Africa: constraints from in situ SHRIMP U-Pb dating of monazite and xenotime. Geology 35, 931–934.
Rasmussen, B., Mueller, A.G., Fletcher, I.R., 2009. Zirconolite and xenotime U–Pb age constraints on the emplacement of the golden mile dolerite sill and gold mineralization at the Mt charlotte mine, Eastern Goldfields Province, Yilgarn Craton, Western Australia. Contrib. Mineral. Petrol. 157, 559–572.
Reich, M., Kesler, S.E., Utsunomiya, S., Palenik, C.S., Chryssoulis, S.L., Ewing, R.C., 2005. Solubility of gold in arsenian pyrite. Geochim. Cosmochim. Acta 69, 2781–2796.
Ressel, M.W., Henry, C.D., 2006. Igneous geology of the Carlin trend, Nevada: development of the Eocene plutonic complex and significance for Carlin-type gold deposits. Econ. Geol. 101, 347–383.
Richards, J.P., 2013. Giant ore deposits formed by optimal alignments and combinations of geological processes. Nat. Geosci. 6, 911–916.
Ridley, J.R., Mengler, F., 2000. Lithological and structural controls on the form and setting of vein stockwork orebodies at the Mount Charlotte gold deposit, Kalgoorlie: Econ. Geol. 95, 85–98.
Sillitoe, R.H., 1994. Erosion and collapse of volcanoes: causes of telescoping in intrusion-centered ore deposits. Geology 22, 945–948.
Sillitoe, R.H., Mortensen, J.K., 2010. Longevity of porphyry copper formation at Quellaveco, Peru. Econ. Geol. 105, 1157–1162.
Simard, M., Gaboury, D., Daigneault, R., Mercier-Langevin, P., 2013. Multistage gold mineralization at the lapa mine, Abitibi Subprovince: insights into auriferous hydrothermal and metasomatic processes in the Cadillac–Larder Lake Fault Zone. Mineral. Deposita 48, 883–905.
Skirrow, R.G., Bastrakov, E.N., Barovich, K., Fraser, G.L., Creaser, R.A., Fanning, C.M., Raymond, O.L., Davidson, G.J., 2007. Timing of iron oxide Cu–Au–(U) hydrothermal activity and Nd isotope constraints on metal sources in the Gawler Craton, South Australia. Econ. Geol. 102, 1441–1470.
Steadman, J.A., Large, R.R., 2014. Pyrite Nodules in Black Shales at the Golden Mile Gold Deposit, Kalgoorlie: Their Geochemistry, Origin, and Significance. Gold14@Kalgoorlie – International Symposium. Curtin University, Kalgoorlie. Australian Institute of Geoscientists, Australia, pp. 115–117.
Steadman, J.A., Large, R.R., Meffre, S., Olin, P.H., Danyushevsky, L.V., Gregory, D.D., Belousov, I., Lounejeva, E., Ireland, T.R., Holden, P., 2015. Synsedimentary to early diagenetic gold in black shale-hosted pyrite nodules at the Golden Mile Deposit, Kalgoorlie, Western Australia. Econ. Geol. 110, 1157–1191.
Stein, H.J., Markey, R.J., Morgan, J.W., Selby, D., Creaser, R.A., McCuaig, T.C., Behn, M., 2001. Re–Os dating of Boddington molybdenite, SW Yilgarn; two Au mineralization events. Record — Australian Geological Survey Organisation, pp. 469–471.
Sung, Y.H., Brugger, J., Ciobanu, C.L., Pring, A., Skinner, W., Nugus, M., 2009. Invisible gold in arsenian pyrite and arsenopyrite from a multistage Archaean gold deposit: Sunrise Dam, Eastern Goldfields Province, Western Australia. Mineral. Deposita 44, 765–791.

Thomas, H.V., Large, R.E., Bull, S.W., Maslennikov, V., Berry, R.F., Fraser, R., Froud, S., Moye, R., 2011. Pyrite and pyrrhotite textures and composition in sediments, laminated quartz veins, and reefs at Bendigo gold mine, Australia: insights for ore genesis. Econ. Geol. 106, 1–31.

Tomich, S.A., 1986. An outline of the economic geology of Kalgoorlie, Western Australia. Trans. Geol. Soc. S. Afr. 89, 35–55.

Tomkins, A.G., 2010. Windows of metamorphic sulfur liberation in the crust: implications for gold deposit genesis. Geochim. Cosmochim. Acta 74, 3246–3259.

Tomkins, A.G., 2013. On the sourc e of orogenic gold. Geology 41, 1255–1256.

Tosdal, R.M., Cline, J.S., Fanning, C.M., Wooden, J.L., 2003. Lead in the Getchell-Turquoise Ridge Carlin-type gold deposits from the perspective of potential igneous and sedimentary rock sources in northern Nevada: implications for fluid and metal sources. Econ. Geol. 98, 1189–1211.

Travis, G.A., Woodall, R., Bartram, G.D., 1971. The geology of the Kalgoorlie Goldfield. Geol. Soc. Aust. Spec. Publ. 3, 175–190.

Vielreicher, N., Groves, D., McNaughton, N., 2014. Late Orogenic Timing of Multiple Styles of Gold Mineralization at Kalgoorlie in a Regional Context. Gold14@Kalgoorlie International Symposium: Extended Abstracts. Australian Institute of Geoscientists.

Vielreicher, N., Groves, D., McNaughton, N., Fletcher, I., 2015. The timing of gold mineralization across the eastern Yilgarn craton using U–Pb geochronology of hydrothermal phosphate minerals. Mineral. Deposita 50, 391–428.

Vielreicher, N.M., Groves, D.I., Snee, L.W., Fletcher, I.R., McNaughton, N.J., 2010. Broad synchroneity of three gold mineralization styles in the Kalgoorlie gold field: SHRIMP, U–Pb, and $^{40}Ar/^{39}Ar$ geochronological evidence. Econ. Geol. 105, 187–227.

Wilson, A.J., Cooke, D.R., Stein, H.J., Fanning, C.M., Holliday, J.R., Tedder, I.J., 2007. U–Pb and Re–Os geochronologic evidence for two alkalic porphyry ore-forming events in the Cadia District, New South Wales, Australia. Econ. Geol. 102, 3–26.

Yakubchuk, A., Stein, H., Wilde, A., 2014. Results of pilot Re–Os dating of sulfides from the Sukhoi log and Olympiada orogenic gold deposits, Russia. Ore Geol. Rev. 59, 21–28.